



# New Late Neolithic (c. 7000–5000 BC) archeointensity data from Syria. Reconstructing 9000years of archeomagnetic field intensity variations in the Middle East

Yves Gallet, Miquel Molist Montaña, Agnès Genevey, Xavier Clop Garcia, Erwan Thébault, Anna Gómez Bach, Maxime Le Goff, Béatrice Robert, Inga Nachasova

## ► To cite this version:

Yves Gallet, Miquel Molist Montaña, Agnès Genevey, Xavier Clop Garcia, Erwan Thébault, et al.. New Late Neolithic (c. 7000–5000 BC) archeointensity data from Syria. Reconstructing 9000years of archeomagnetic field intensity variations in the Middle East. Physics of the Earth and Planetary Interiors, 2015, 238, pp.89-103. 10.1016/j.pepi.2014.11.003 . hal-01096917

**HAL Id: hal-01096917**

**<https://hal.sorbonne-universite.fr/hal-01096917>**

Submitted on 18 Dec 2014

**HAL** is a multi-disciplinary open access archive for the deposit and dissemination of scientific research documents, whether they are published or not. The documents may come from teaching and research institutions in France or abroad, or from public or private research centers.

L'archive ouverte pluridisciplinaire **HAL**, est destinée au dépôt et à la diffusion de documents scientifiques de niveau recherche, publiés ou non, émanant des établissements d'enseignement et de recherche français ou étrangers, des laboratoires publics ou privés.

**New Late Neolithic (c.7000-5000 BC) archeointensity data from Syria.  
Reconstructing 9000 years of archeomagnetic field intensity variations in the  
Middle East**

Yves Gallet <sup>a</sup>, Miquel Molist Montaña <sup>b</sup>, Agnès Genevey <sup>c</sup>, Xavier Clop García <sup>b</sup>, Erwan  
Thébault <sup>a,d</sup>, Anna Gómez Bach <sup>b</sup>, Maxime Le Goff <sup>a</sup>, Béatrice Robert <sup>e</sup>, Inga Nachasova <sup>f</sup>

<sup>a</sup> *Institut de Physique du Globe de Paris, Sorbonne Paris Cité, Université Paris Diderot, UMR  
7154 CNRS, F-75005 Paris, France*

<sup>b</sup> *SGR SAPPO. Prehistory Department, Facultat de Filosofia i Lletres, Edifici B, Universitat  
Autònoma de Barcelona 08193 Bellaterra, Barcelona, Spain*

<sup>c</sup> *UPMC Université Paris 06, UMR CNRS 8220, Laboratoire d'Archéologie Moléculaire et  
Structurale, LAMS, F-75005 Paris, France*

<sup>d</sup> *LPG, UMR CNRS 6112, Laboratoire de Planétologie et Géodynamique de Nantes,  
Université de Nantes, 44322 Nantes cedex 03, France*

<sup>e</sup> *Université Lumière – Lyon 2, UMR CNRS 5133 ArchéOrient, Lyon, France*

<sup>f</sup> *Institute of Physics of the Earth, Russian Academy of Science, Moscow, Russia*

**Keywords:** Archeomagnetism, Geomagnetic field intensity, Neolithic, Halaf, Middle East,  
Holocene

**ABSTRACT**

We present new archeomagnetic intensity data from two Late Neolithic archeological  
sites (Tell Halula and Tell Masaikh) in Syria. These data, from 24 groups of potsherds  
encompassing 15 different time levels, are obtained using the Triaxe experimental  
protocol, which takes into account both the thermoremanent magnetization anisotropy  
and cooling rate effects on intensity determinations. They allow us to recover the  
geomagnetic intensity variations in the Middle East, between ~7000 BC and ~5000 BC,  
i.e. during the so-called pre-Halaf, proto-Halaf, Halaf and Halaf-Ubaid Transitional  
cultural phases. The data are compared with previous archeointensity results of similar  
ages from Northern Iraq (Yarim Tepe II and Tell Sotto) and Bulgaria. We find that  
previous dating of the Iraqi material was in error. When corrected, all northern  
Mesopotamian data show a relatively good consistency and also reasonably match with  
the Bulgarian archeointensity dataset. Using a compilation of available data, we  
construct a geomagnetic field intensity variation curve for the Middle East  
encompassing the past 9000 years, which makes it presently the longest known regional  
archeomagnetic intensity record. We further use this compilation to constrain variations

in dipole field moment over most of the Holocene. In particular, we discuss the possibility that a significant dipole moment maximum occurred during the third millennium BC, which cannot easily be identified in available time-varying global geomagnetic field reconstructions.

## 1. Introduction

Recent studies have been focused on the construction of time-varying global archeomagnetic field models that cover most of the Holocene (e.g. Korte et al., 2011; Nilsson et al., 2014; Pavón-Carrasco et al., 2014). These models have been developed with the aim to decipher core dynamics over centennial and millennial time scales, the evolution of the past solar activity and the interactions between geomagnetic field and external processes (e.g. Korte et al., 2009; Licht et al., 2013; Usoskin et al., 2014). In all these studies, however, the authors acknowledge the fact that for the more ancient periods, i.e. beyond the first millennium BC, the reliability and accuracy of the geomagnetic field models are strongly penalized by the low number and the poor temporal and geographical distributions of the available archeomagnetic and volcanic paleomagnetic data. To overcome this problem, often paleomagnetic data from sediments have been included in the models reference dataset; nevertheless sedimentary data do not significantly improve the accuracy of the models because a part of them, difficult to estimate, may be biased by experimental errors and/or because these data often lack precise dating (e.g. Valet et al., 2008; Nilsson et al., 2010). There is therefore a critical need for new well dated archeomagnetic data dated with ages older than the first millennium BC.

The Middle East, thanks to its rich archeological and historical heritage, offers the possibility to travel back through the geomagnetic field history over most of the Holocene, recovering what could be the longest known archeomagnetic field record. Archeomagnetic studies conducted up to now were mainly focused on the Bronze and Iron Age archeological periods, allowing a better characterization of the regional geomagnetic field intensity behavior for the last 3 millennia BC (i.e. Genevey et al., 2003; Gallet and Le Goff, 2006; Gallet et al., 2008, 2014; Ben-Yosef et al., 2008, 2009; Gallet and Al Maqdissi, 2010; Thébaud and Gallet, 2010; Shaar et al., 2011; Ertepinar et al., 2012; Gallet and Butterlin, 2014). These studies have revealed significant field intensity

variations, and in particular a series of intensity maxima between ~2600 and 2500 BC, between ~2300-2000 BC, around 1500 BC and at the very beginning of the first millennium BC (e.g. Gallet et al., 2014). These studies have further shown that the beginning of the first millennium BC was most probably marked by the highest geomagnetic field intensity so far detected during the Holocene and perhaps even before (Ben-Yosef et al., 2009; Shaar et al., 2011; Ertepinar et al., 2012; Livermore et al., 2014).

In contrast, for older periods between ~7000 BC and 3000 BC, i.e. during the Late Neolithic (or Pottery Neolithic) and the Chalcolithic, the archeointensity data from the Middle East remain relatively scarce, which prevents an accurate description of the regional geomagnetic field intensity variations (e.g. Genevey et al., 2003; Ben-Yosef et al., 2008). However, several possibilities exist to sample pre-Bronze Age archeological sites. This is particularly true for the 6th millennium BC, which saw the development of the Halaf culture throughout the northern Mesopotamian region. This culture was named after the Tell Halaf archeological site in northern Syria (Fig. 1a), which was discovered and first excavated by the German diplomat Max von Oppenheim at the beginning of the 20th century. The Halaf culture is notably characterized by a plentiful pottery production presenting a fine and light-colored clay paste, with brown or black monochrome or polychromatic painted decorations (e.g. Akkermans and Schwartz, 2003; Nieuwenhuyse et al., 2013 and references therein). This well-fired ceramic production thus constitutes a promising target for archeointensity investigations.

Going further back in time, archeomagnetic studies may benefit from recent archeological studies conducted in Syria that focused on the 7th millennium BC, which saw the emergence of the first pottery production in the Near East (e.g. Tsuneki and Miyake, 1996; Le Mièrre and Picon, 1998; Nishiaki and Le Mièrre, 2005; Molist et al., 2007; Nieuwenhuyse et al., 2010, 2013). At first rare, the pottery was sometimes of a surprisingly elaborated conception with a painted decoration during a primitive phase referred to as the "Initial Pottery Neolithic" (~7000-6700 BC; e.g. Van der Plicht et al., 2011). By the middle of the 7th millennium BC, the use of ceramics spread over northern Mesopotamia (Nieuwenhuyse et al., 2010, 2013 and references therein). This pre-Halaf period is mainly represented by undecorated plant-tempered pottery with a coarse clay paste shaped into baskets. The fineness of the clay paste improved at the end of the 7th millennium BC during a period referred to as proto-Halaf (~6050-5900 BC), just



preceding the Halaf period, with the use of mineral-tempered clay (e.g. Cruells and Nieuwenhuyse, 2004). According to Akkermans and Schwarz (2003), the pre-Halaf coarse pottery was produced in open fires, with heating temperatures of about 700-750°C, while the elaborate Halaf ceramics were most probably heated at higher temperatures in chambered kilns. For the pre- and proto-Halaf periods encompassing the 7th millennium BC, archeointensity studies are thus still possible, but they may be further complicated by the characteristics of the ceramic production.

To extend the Syrian geomagnetic field intensity record, which presently mainly documents the Bronze and Iron Age periods, we conducted an archeomagnetic study on the pre-Halaf, proto-Halaf, Halaf and Halaf-Ubaid Transitional archeological periods, a time interval of nearly two millennia (~7000 to ~5000 BC) covering the Pottery Neolithic, at the end of the Neolithic (e.g. Campbell, 2007; Campbell and Fletcher, 2010; Van der Plicht et al., 2011; Nieuwenhuyse et al., 2013 and references therein). The new archeointensity data reported in this study were mostly obtained from potsherds collected from the archeological site of Tell Halula located in northern Syria (Fig. 1a). These results were complemented by few data obtained from potsherds discovered at the archeological site of Tell Masaikh, located south-east along the middle course of the Euphrates river (Fig. 1a). It is of interest to note that the longest and almost continuous regional archeointensity record presently available was obtained from Bulgaria (Kovacheva et al., 2014). It begins around 6000 BC, i.e. a date during the proto-Halaf period, which means that some of the new data presented in this study are the oldest archeointensity data recovered until now. Furthermore, we recall the recent effort of data compilation of archeomagnetic, volcanic and sedimentary paleomagnetic results that led to the construction of global archeomagnetic field models encompassing almost the entire Holocene (Korte et al., 2011; Nilsson et al., 2014; Pavón-Carrasco et al., 2014). Any new archeomagnetic intensity data dated to the Late Neolithic-Early Chalcolithic period, now rather rare (e.g. Genevey et al., 2008; Knudsen et al., 2008), will therefore allow us to test, at least regionally, the accuracy of the available models and in return will better constrain these models. This point is particularly critical and we will also report in this study on erroneous dating of a relatively large archeointensity dataset previously obtained in the Middle East for the 7<sup>th</sup> and 6<sup>th</sup> millennia BC (Nachasova and Burakov, 1995, 1998).

## 2. Archeomagnetic sampling

### 2.1. *Tell Halula*

Tell Halula ( $\lambda=36^{\circ}25'N$ ,  $\varphi=38^{\circ}10'E$ ) is located in the modern Syrian administrative province of Raqqqa, about 80 km west of the city of Raqqqa and 85 km east of the city of Aleppo. This archeological site, ~4 km west of the Euphrates, forms a sub-circular artificial mound (360 m x 300 m), with an archeological deposit thickness of ~14 m (Fig. 1b). Archeological excavations conducted since 1991 by a team of the Universitat Aut3noma de Barcelona revealed a total of 38 phases of occupation. From the stratigraphic and archeological constraints (including chipped stone artefacts, pottery typology, figurines and architecture), it has been determined that the site was occupied continuously from the Middle Pre-Pottery Neolithic B (PPNB) to the Late Halaf periods, i.e. from ~7800 to 5300 cal BC (Molist et al. 2007, 2013; Molist 1996, 2001). The systematic archeological fieldwork at Tell Halula has brought significant knowledge about the development of farming, especially in the final stages of the Neolithisation process, when economic, technological and cultural changes were being consolidated.

The different phases of human occupation have been recovered in several sectors, especially in the south, south-east and central parts of the settlement (Sectors 1, 2, 7, 14, 30, 44 and 45). The Neolithic ceramic horizon encompasses most of the seventh millennium BC and part of the sixth millennium BC (Architectural Phases 20 to 38), spanning the pre-Halaf (or Period 5 according to Lyon's School terminology; Hours et al., 1994), the proto-Halaf or Halaf Transitional and the Halaf (Early, Middle, Late) periods. The archeological and stratigraphic data indicate the presence of a sedentary population, with several large houses or architectural structures relatively dispersed over a surface of ~6 ha, i.e. with large open areas between households and buildings for domestic use. Furthermore, several structures for a collective use were discovered for the pre-Halaf period, with a massive enclosing wall in Sector 1 and a drainage channel in Sector SS7 (Molist, 1996, 1998; Molist and Faura, 1999; Molist et al., 2013).

The pottery assemblages analyzed in the present study were sampled following the main chronocultural phases documented at Tell Halula (Fig. 2; see description in Molist et al., 2013 and Supplementary Text1). Here, we used the same chronological

time scale as in Molist et al. (2013). For the first pottery production within the Early Pre-Halaf (Ceramic Phase I; ~7000-6600 BC), two groups of fragments collected from the top of Sector 2 were analyzed. The first group of fragments (SY 127) was recovered from a pit located in an open area and the second (SY 125), a little younger than the previous one, was collected from an occupation level associated with a rectangular building. For the intermediate pre-Halaf period (Ceramic Phase II; ~6600-6300 BC), three pottery groups were collected from a large outdoor space between several domestic units. Their age assignment was established via stratigraphy, with the group of potsherds SY96 being the most recent, SY97-129 intermediate and SY98-128 being the oldest. Finally, pottery group SY130, comprising pottery fragments found in a pit from Sector 49, comes from the late pre-Halaf (Ceramic Phase III; ~6300-6050 BC).

For the period referred to as proto-Halaf (~6050-5900 BC), corresponding to Ceramic Phase IV defined at Tell Halula, two pottery groups of household artifacts were collected in Sectors 44 (SY94-137) and 40 (SY95). A single group (SY91) lies within the Early Halaf period (Ceramic Phase V; ~5900-5750 BC), which was recovered from a multicellular house located in sector 44. Different pits discovered in the same area of Sector 45 yielded four contemporaneous groups of pottery (SY87, SY88, SY89, SY90) dated within the Middle Halaf period (Ceramic Phase VI; ~5750-5550 BC).

Nine groups of fragments were collected from the most recent chronological phases at Tell Halula dated in the Late Halaf (Ceramic Phase VII; ~5550-5300 BC). This relatively dense sampling was possible due to a relatively complete stratigraphic sequence from Sector 49 (Gómez, 2011). For most of these groups, the fragments were recovered from different pits excavated in a large open yard, that were used for the disposal of ash and domestic waste. The stratigraphic data and the ceramic typology distinguish five successive temporal intervals, each being documented by one or several pottery groups (from older to younger: SY86-131; SY135; SY84 and SY138; SY82 and SY83-136; SY80, SY81 and SY132).

In summary, 22 different pottery groups from 14 successive occupation levels were thus sampled at Tell Halula, whose dates span ~1700 years, between ~7000 and ~5300 BC. For displaying the results in a relative chronological framework for phases II and VII, we made the rough approximation of an equi-temporal distribution for respectively the three and five successive occupation levels (i.e. assuming a duration of

100 years for each intermediate pre-Halaf level between 6600 BC and 6300 BC and a duration of 50 years for each Late Halaf level between 5550 BC and 5300 BC; dating with \* in Table 1).

## 2.2. Tell Masaikh

The archeological site of Tell Masaikh ( $\lambda=34^{\circ}25'N$ ,  $\varphi=40^{\circ}01'E$ ) is located on a river terrace in the middle Euphrates Valley (left bank), in the modern province of Deir ez-Zor (eastern Syria). Discovered in 1996 by the *Mission Archéologique Française de Ashara/Terqa* led by O. Rouault, excavations at Tell Masaikh (~4 km from Terqa), conducted under the leadership of M.-G. Masetti-Rouault, have revealed several phases of occupation starting with the Late Neolithic (Halaf). More recent periods include significant Neo-Assyrian remains, with a citadel and a palace dated in the 9<sup>th</sup>-8<sup>th</sup> centuries BC (Iron Age period), which led the identification of Tell Masaikh as the Assyrian city named Kar-Assurnasirpal (see general discussion in Masetti-Rouault, 2010).

The discovery in the western sector D of Tell Masaikh of an artisanal Halaf settlement makes this site also quite unique. It is located away from most other known Halaf archeological sites situated more to the North with rainfall above 250 mm/year (while rainfall is below this isohyet in the Tell Masaikh region; e.g. Masetti-Rouault, 2006; Robert, 2010), which opens discussion on farming systems and on the use of irrigation at this time.

Excavations of the Halaf levels at Tell Masaikh unearthed several occupation levels in open areas with fire places (tannurs), several kilns probably for pottery production and a 1.5 m-thick, ~20 m-long stone wall that supported a terrace. A rich ensemble of Late Halaf potsherds was also recovered. The potsherds analyzed in the present study were found in the uppermost layers dated in the Halaf-Ubaid Transitional (~5300-5000 BC; e.g. Campbell and Fletcher, 2010) based on their typology and from the painted decoration that used manganese pigments for black color. The youngest Halaf pottery belongs to polychrome Late Halaf types associated with some Impressed Ware known as Dalma types and Ubaid-style ceramics (Masetti-Rouault, 2005; Robert et al., 2008; Robert, 2010). We sampled in Locus K171 two groups of these fragments with

fine mineral-tempered clay paste (pottery groups SY37, SY38), the first in the occupation layer referred to as E2, and the second on floor E7 on top of layer E2.

### 3. New archeomagnetic intensity results

All the archeointensity measurements reported in this study were obtained using the experimental protocol developed by Le Goff and Gallet (2004) for the Triaxe magnetometer. The details of this experimental protocol can be found in Le Goff and Gallet (2004) (see also Genevey et al., 2009; 2013; Hartmann et al., 2010; Gallet et al., 2014). We only recall here that it relies on magnetization measurements of a small specimen ( $<1\text{cm}^3$ ) directly carried out at high temperatures and on a sequence of measurements (with successive heating and cooling cycles) automatically performed over a fixed temperature range between a low temperature referred to as  $T_1$  (typically of  $150^\circ\text{C}$ ) and a high temperature referred to as  $T_2$  (typically between  $500^\circ\text{C}$  and  $530^\circ\text{C}$ ). In the past few years, a relatively large collection of archeointensity data of different ages and of different origins was obtained using the Triaxe, and comparative studies with results derived from more classical methods (i.e. from the Thellier and Thellier's (1959) method as revised by Coe (1967) or from the IZZI version of Thellier and Thellier's (1959) method; e.g. Yu et al., 2004) demonstrated the reliability of the Triaxe intensity data when quality criteria are taken into account. In our study, we use the same quality criteria relative to the intensity determination for a specimen as those described by Genevey et al. (2009) and Hartmann et al. (2010, 2011), and which were also used more recently by Genevey et al. (2013), Gallet et al. (2014) and Gallet and Butterlin (2014) (Supplementary Table 1). In particular, these criteria allow us to eliminate the data that could be biased due to alteration of the magnetic minerals during heating. Moreover, the temperature range over which the intensity determinations are recovered from each specimen is precisely adjusted so that the analyzed magnetization component is univectorial and corresponds to the magnetization acquired during the manufacture of the pottery. Fig. 3 shows two examples of demagnetization behaviors. After the removal of the viscous low-temperature component, the first behavior shows a single magnetization component above  $\sim 200^\circ\text{C}$  (SY89-08), while the second behavior reveals two components (SY140-06). In these cases, the temperature range was adjusted above  $\sim 200^\circ\text{C}$  and  $\sim 340^\circ\text{C}$ , respectively for obtaining intensity determinations

at the specimen level. Finally, the intensity data should not be affected by the presence of multidomain magnetite grains and they take into account both the thermoremanent magnetization (TRM) anisotropy and cooling rate effects on TRM acquisition (for a thorough discussion on these aspects, see for instance in Le Goff and Gallet, 2004; Genevey et al., 2008, 2009; Hartmann et al., 2010).

Our archeointensity analyses were complemented by hysteresis measurements and by isothermal remanent magnetization (IRM) acquisition up to 0.8 T performed at Saint Maur using a laboratory-built inductometer coupled with an electro-magnet. In most cases, two fragments were analyzed for each group of fragments. IRM measurements show very similar behaviors with saturation reached in relatively low magnetic fields ( $\sim 0.2\text{--}0.3$  T), indicating the absence of high-coercivity minerals (Fig. 4a). We note that the hysteresis loops are generally not constricted (Fig. 4b-c). Thermomagnetic low-field susceptibility curves obtained using a KLY-3 Kappabridge coupled with a CS3 thermal unit show that the existing magnetic grains have maximum unblocking temperatures below  $600^\circ\text{C}$  (Fig. 4d-g). All these magnetic properties indicate that the magnetization of our specimens is most probably predominantly carried by minerals of the (titano)magnetite family. Furthermore, the thermomagnetic curves exhibit variable behaviors, independently of the age of the fragments, which suggests the presence of (titano)magnetite with different titanium contents or different grain sizes. We also observe a good reversibility between the heating and cooling susceptibility vs. temperature curves, which constitutes a good marker of the stability of the magnetic mineralogy on heating. We note that these magnetic properties are very similar to those we previously obtained from Syrian fired-clay artifacts of younger ages (e.g. Genevey et al., 2003; Gallet et al., 2008; 2014; Gallet and Butterlin, 2014).

Except for one case, the hysteresis parameters obtained for the fragments from Tell Halula lie within the pseudo-single domain (PSD) range of magnetite defined by Dunlop et al. (2002a) when projected on a Day plot (Day et al., 1977). Most  $M_{\text{RS}}/M_{\text{S}}$  and  $H_{\text{CR}}/H_{\text{C}}$  ratios are concentrated inside a restricted area, with  $\sim 0.30 > M_{\text{RS}}/M_{\text{S}} > \sim 0.15$  and  $\sim 4 > H_{\text{CR}}/H_{\text{C}} > \sim 2.5$ , above the theoretical mixing curves for mixture of SD and MD magnetite grains but also well below the mixing curve of SD and superparamagnetic (SP) magnetite grains (Fig. 4h). According to Dunlop (2002b), this may reflect a large distribution of grain sizes, including SP, SD and MD magnetite grains. In contrast, most

of the hysteresis parameters obtained from Tell Masaikh (open blue triangles in Fig. 4h) fall within the theoretical SD-MD mixing curves defined by Dunlop (2002a), therefore indicating a coarser grain size distribution for those specimens. It is worth mentioning that the evolution of the techniques (preparation of the clay paste, firing conditions) used to produce ceramics at Tell Halula between the pre-Halaf and Halaf periods is clearly not reflected in the hysteresis ratios, their dispersions being very similar regardless of the age of the fragments (colored symbols in Fig. 4h). Further considering the data from Tell Masaikh and the previous ones obtained from Ebla/Tell Mardikh (grey dots in Fig. 4h; Gallet et al., 2014), it appears that the distribution of the hysteresis parameters obtained at a given archeological site constitutes a magnetic signature of the clay source used to produce pottery at this site, and it may be used as an identification tool complementary to more classical chemical analyses.

Fig. 5 shows the intensity results obtained from eight pottery groups. Each curve from each panel shown in this figure exhibits the intensity data obtained for one specimen over a temperature range often exceeding 200-250°C. In general, we only analyzed one specimen per fragment. However, when the number of favorable fragments was  $\leq 5$  (i.e. for pottery groups SY127, SY125, SY95, SY38), we analyzed three specimens from each fragment and we first estimated a mean intensity value at the fragment level before computing a mean value at the group level. The success rate of our archeointensity analyses significantly varies according to the archeological periods. While it is only 36% for the pre-Halaf period (54 fragments from 151 analyzed fragments) and 56 % (22 from 39 fragments) for the proto-Halaf period, it increases up to 70% for the sites dated in the Halaf period (133 from 191 fragments) and 67% for the Halaf-Ubaid Transitional period (16 favorable fragments from 24 studied fragments). The relatively low success rate for the pre-Halaf fragments is mainly due to the presence of two magnetization components, which is likely related to the use of these ceramics for cooking (hence preventing in many cases the clear isolation of a primary magnetization). Examples of failed results are reported in Supplementary Fig. 1. Overall, we analyzed a total of 405 fragments, among which 225 fragments (254 specimens) yielded favorable archeointensity results, allowing us to determine 24 mean intensity values at the pottery group level. Results obtained at the specimen/fragment level are detailed in Supplementary Table 2, while Table 1 provides the group-mean intensity values. These intensity values are generally well defined, with a number of fragments

analyzed per site larger or equal to 7 for 19 pottery groups ( $\geq 10$  for 10 sites) and a standard deviation always of less than 5  $\mu\text{T}$ , ranging between 1.8 % and 11.4 % of the corresponding group-mean intensity values ( $\leq 5.0$  % for 10 sites and  $\leq 7.5$  % for 21 among the 24 studied pottery groups). We note, however, that the mean intensity value obtained for group SY125 (~6650-6550 BC) is only defined by two fragments (6 specimens), but it was kept for the discussion below because of the scarcity of such old archeointensity data.

#### 4. Late Neolithic archeointensity variations in the Middle East

The new archeointensity data are reported in Fig. 6 (see also Supplementary Fig. 2, where the results are averaged over the successive occupation levels). The new results show that the time interval between ~7000 BC and ~5000 BC was apparently marked in the Middle East by an overall decreasing trend in geomagnetic field intensity. This decrease was however not regular. In particular, a relative intensity minimum is observed at the beginning of the Late Halaf period (pottery group SY86-131 with 20 favorable fragments), around the middle of the 6th millennium BC. An intensity peak appears to have occurred during the Late Halaf period, between ~5550 and ~5300 BC. This intensity peak is supported by the low geomagnetic field intensity values obtained at Tell Masaikh for the Halaf-Ubaid Transitional period.

We compared the new Tell Halula and Tell Masaikh data with two other archeointensity datasets of the same age previously obtained in relatively nearby regions (Fig. 7). The first dataset includes results obtained at Yarim Tepe II and Tell Sotto, two multi-level archeological sites from northern Iraq (Fig. 1a; Nachasova and Burakov, 1995, 1998). In these two studies, the pottery fragments were selected and dated according to their stratigraphic position within a sequence of archeological deposits (with a total thickness of 780 cm at Yarim Tepe II and 280 cm at Tell Sotto), and assuming a constant accumulation rate of archeological deposits. Although such a sampling procedure may obviously introduce large uncertainties in the dating of the studied fragments, it nevertheless appears that this approach can provide satisfactory results (e.g. Nachasova and Burakov, 1998; Kostadinova-Avramova et al., 2014). However, in both cases, the dating considered by Nachasova and Burakov (1995, 1998)



appears systematically shifted by several centuries relative to the most recent chronological Pottery Neolithic time scale (see Campbell, 2007; Bernbeck and Nieuwenhuyse, 2013). Indeed, the fragments from Yarim Tepe II are unambiguously archeologically dated to the Middle-Late Halaf period (~5750-5300 BC; e.g., Campbell, 2007; Robert, 2009; Bernbeck and Nieuwenhuyse, 2013 and references therein), but their ages were mostly assigned in the 5th millennium BC. Similarly, the fragments collected at Tell Sotto were dated to the middle of the 6th millennium BC by Nachasova and Burakov (1998), but the studied ceramics are dated to the Late Pre-Halaf (Late proto-Hassuna and Archaic Hassuna cultural phases), i.e. between ~6400 and ~6050 BC (e.g. Bader, 1989; Bader and Le Mière, 2013; Le Mière pers. comm. 2014).

For these reasons, we assigned new ages to Yarim Tepe II and Tell Sotto considering first, the stratigraphic position of the concerned fragments as provided by the authors and second, assuming that the entire Middle-Late Halaf and Late Pre-Halaf periods were represented in the Yarim Tepe II and Tell Sotto deposits (like the authors considered but for two other time intervals). Finally, for displaying in Fig. 7a the data obtained at Yarim Tepe II, with only a single specimen studied per fragment, and at Tell Sotto we also performed intensity averaging over several fragments when the latter come from the same stratigraphic intervals, i.e. each time there was a group of fragments considered of the same age. We observe an overall good agreement with the data obtained at Tell Halula and Tell Masaikh. In particular, this agreement confirms the occurrence in northern Mesopotamia of a relative intensity minimum around the middle of the 6th millennium BC, which further strengthens the occurrence of an intensity peak at the beginning of the second half of the 6th millennium BC.

The second archeointensity dataset comprises the results encompassing the 6th millennium BC from Bulgaria that were recently updated by Kovacheva et al. (2014) (Fig. 7b). From this new analysis, a century-scale intensity peak seems to be emerging around the middle of the 6<sup>th</sup> millennium, which might coincide, within age uncertainties, with that observed from the Syrian Late Halaf data. According to this interpretation, the data available for the Halaf-Ubaid Transitional period would come prior to the geomagnetic field intensity increase observed in the Bulgarian data at the end of the 6<sup>th</sup> millennium BC. Constraining further this preliminary correlation will require the acquisition of new archeointensity data in the Balkans and in the Middle East.

## 5. Discussion

We have undertaken the construction of a geomagnetic field intensity secular variation curve in the Middle East during the Holocene. For this purpose, we selected all the archeointensity data available inside a circle with a radius 1000 km around the archeological site of Tell Halaf ( $\lambda=36^{\circ}49'N$ ,  $\varphi=40^{\circ}02'E$ ; Supplementary Fig. 3). The data were retrieved from the ArcheoInt database (Genevey et al., 2008) and complemented with the more recent studies (Ben-Yosef et al., 2009; Gallet and Al Maqdissi, 2010; Shaar et al., 2011, 2014; Ertepinar et al., 2012; Gallet et al., 2014; Gallet and Butterlin, 2014). They were obtained from the eastern part of Turkey, Cyprus, Syria, the Levant, Iraq, from the western part of Iran and from the Caucasus. Note that the large dataset from the Balkans and Greece (e.g. De Marco et al., 2008; Tema and Kondopoulou, 2011; Kovacheva et al., 2014) has not been included to allow it to be compared to different regional secular variation behaviors from elsewhere (e.g. between the Middle East, Eastern Europe and Western Europe). Genevey et al. (2008) proposed a set of selection criteria in order to distinguish between all available data those that meet minimum quality criteria. This approach enabled the construction of two datasets referred to as "Selected data" and "All data" in Genevey et al. (2008). Hereafter we have considered the compilation of selected data to calculate the Middle East geomagnetic field intensity variation curve, considering the new dating we estimated for Tell Sotto and Yarim Tepe II and using, for these two sites, the mean intensity values computed from fragments associated with the same stratigraphic level (Fig. 7a).

To calculate our curve, we first applied a method based on the use of sliding windows of 200 years successively shifted by 10 years through the past 9 millennia. We computed VADM values only for those time intervals containing at least 3 results. Following Thébaud and Gallet (2010) and Licht et al. (2013), we also used the bootstrap technique with 1000 runs by introducing random noise in the data within their experimental and age uncertainties. This allowed us to compute 1000 intensity variation curves. In Fig. 8a we displayed the averaged VADM (thick line) together with the minimum and maximum VADM values obtained for the different sliding windows, hence defining an envelope of equally possible VADM values. Due to the insufficient number of archeointensity data spanning the 5th and 4th millennia BC, no averaged curve could be

determined between ~4930 BC and ~3650 BC, i.e. during the Ubaid and Uruk periods in Mesopotamia. This time interval therefore constitutes a particularly important target for future archeomagnetic studies in the Middle East. For other periods, the computed curve appears very consistent with almost all the Syrian data (blue dots in Fig. 8a; Genevey et al., 2003; Gallet and Le Goff, 2006; Gallet et al., 2006, 2008, 2014; Gallet and Al Maqdisi, 2010; Gallet and Butterlin, 2014 and this study). We observe the same variation trends, with distinct intensity maxima during the second half of the first millennium AD, at the beginning of the first millennium BC and around the middle of the third millennium BC. Supplementary Fig. 4 also exhibits the averaged intensity curve computed without the Syrian data, showing in particular that the latter data set allows us to better constrain the curve during the third millennium BC (note that this curve takes into account the new dating of the Tell Sotto and Yarim Tepe II data). The temporal resolution of 200 years of the regional averaged curve most probably prevents the recovery of distinct century-scale intensity (VADM) maxima at ~1500 BC, ~2550 BC and ~2300 BC clearly observed from Syrian data at Ebla and Mari (Gallet et al., 2008, 2014; Gallet and Butterlin, 2014), as well as the maximum in intensity between ~5500 and ~5300 BC exhibited by the Tell Halula data or the spike events proposed by Ben-Yosef et al. (2009) and Shaar et al. (2011) at the very beginning of the first millennium BC.

The second approach is similar to the method described above but relies on the more complex cubic B-splines time parameterization and uses an iterative scheme to identify and then to weight the data that are considered as outliers (Fig. 8b; modified from Thébault and Gallet, 2010). The algorithm first proposes a set of possible spline knots irregularly spaced. The spacing is designed to take full advantage of the varying time resolution between epochs that arises from the uneven time distribution of the reference archeomagnetic data. For instance, it is found that the maximum achievable time resolution is about 150 years between 7000 BC to about 5000 BC and between ~3000 BC and 2000 AD, while searching for features with time resolution lower than 800 years makes little sense between ~5000 BC and ~3000 BC. Then, the data are as before 1000 times randomly noised within their a priori error bars. For each curve, the algorithm checks whether the maximum likelihood solution belongs to the a priori 95% error bar of the data and weights accordingly the data that are systematically outside this confidence interval. Fig. 8b displays the final solution with the maximum probability

in black and its 95% fluctuation envelope in light blue. This envelope contains 95% of the maximum likelihood curves estimated by the bootstrap for the 1000 iterations, and it highlights the variability between the different curves. This parameter is important for testing the precision of the most probable curve and for identifying the fine time variations that persist after resampling. Formally, however, the statistical significance of a time variation can be assessed only after the computation of the 95% confidence interval (in red) that is traditionally calculated *a posteriori* from the misfit function between the data and the ensemble of models. Compared to the first approach, the likelihood solution provided in supplementary Table 3 is generally smoother. This feature is desired for testing whether the apparent fine time variation of the maximum likelihood can be considered as robust. A striking feature emerging from the comparison between Fig. 8a and Fig. 8b is that the final solution is independent of the chosen modeling scheme. This is seemingly positive evidence that the observed magnetic field intensity variations are well constrained (within the given time resolution) by the available data in the chosen geographical area.

We then sought to constrain the variations in global geomagnetic dipole field moment over the past 9 millennia. For this, we averaged the archeointensity data available in the Middle East over sliding windows of 500 years, roughly assuming that this rather long duration may suffice to average out most of the non-dipole contributions (e.g. Hulot and Le Mouél, 1994; Genevey et al., 2008; Knudsen et al., 2008). On the other hand, this averaging smoothes out the more rapid variations in dipole moment over centennial time scales (Genevey et al., 2009; 2013). The curve constructed using the same technique as in Fig. 8a is shown in Fig. 9a, together with the VADM computed by Knudsen et al. (2008) using the global GEOMAGIA50 database (Korhonen et al., 2008) and applying both temporal and geographical averaging to eliminate the non-dipole components. As a general comment, the two curves exhibit the same dipole behavior during the past three millennia (although the magnitude and the amplitude of the variations are not strictly the same), characterized by two periods of stronger dipole moment during the first millennium BC and during the second half of the first millennium AD (see also Genevey et al., 2008; Hong et al., 2013). In contrast, these curves are significantly different during the third millennium BC, with a smooth VADM evolution in the case of the Knudsen et al. (2008) curve but with a distinct dipole maximum in our Middle East curve. For older periods, there is again a good consistency

between the two curves, but we note the large error bars of Knudsen et al.'s (2008) curve for the 7th-6th millennium segment. Thus the question remains as to the significance of the dipole maximum observed in the Middle East during the third millennium BC, which is well constrained by a significant number of data. Owing to the rather good agreement between the two curves, especially during the past three millennia, the VADM maximum we observe during the third millennium BC might well be a global (dipole) geomagnetic feature that requires further confirmation. If true, it would indicate that the dipole evolution varied more erratically than previously thought, with an oscillatory behavior at least between  $\sim 3000$  BC and 2000 AD of typical time scale of about 1700 years (see also Burakov et al., 1998).

Fig. 9b compares our VADM variation curve with dipole moments derived from global geomagnetic field modeling that was recently constructed using only archeomagnetic and volcanic data (Pavón-Carrasco et al., 2014, in blue) and another that also incorporated paleomagnetic data from sediments (Nilsson et al., 2014 in orange and green; note that this latter reconstruction supersedes the previous field reconstruction of Korte et al., 2011). The field models that partly rely on sediment data naturally show time variations smoother than that of the models constructed using only the archeomagnetic and volcanic data. Hence, the dipole moments derived by Nilsson et al. (2014) during the 7th millennium BC are lower than the ones proposed by Pavón-Carrasco et al. (2014) and lower than the averaged VADM we estimated from the Middle East. However, at the beginning of the first millennium BC, the VADM values from the Middle East are much higher than the dipole moments from either models. Neither of two reconstructions shows the distinct dipole maxima previously observed during the past three millennia (Fig. 9a; Genevey et al., 2008; Knudsen et al., 2008), in particular the one dated to the first millennium AD. This clearly poses the question of the consistency between the VADM estimates and the time-varying dipole moment reconstructions. Nevertheless, it could be argued that the field modeling of Pavón-Carrasco et al. (2014) gives some support to the occurrence of a dipole moment maximum during the third millennium BC (Fig. 9b). Such an agreement still needs to be confirmed because the proposed field reconstruction shows numerous centennial-scale fluctuations with similar amplitudes over the entire sequence, a feature whose geomagnetic origin is questionable.

As a concluding remark, we point out that the different time-varying archeomagnetic field reconstructions encompassing the 7th-5th millennium time interval all suffer from the erroneous dating affecting the Yarim Tepe II and Tell Sotto data. Together with the corrected Yarim Tepe II and Tell Sotto ages, the new archeointensity data obtained in the present study dated to between 7000 BC and 5000 BC will help improve the reliability of the next generation of geomagnetic field models spanning the Late Neolithic period. Besides implications for geomagnetism, this improvement may be of particular interest in providing chronological time constraints for archeological purposes, during a fascinating period (e.g. Berger and Guilaine, 2009) that was marked by the beginning of the Neolithic expansion from the Middle East toward Western Europe.

## Acknowledgements

We thank Michel Al Maqdissi (DGAM, Damascus), who made possible this archeomagnetic study. We are also grateful to Stuart Gilder and 2 anonymous reviewers for helpful comments on the manuscript. Y.G. and I.N. were partly financed by grant of the Russian Ministry of Science and Education N 14.Z50.31.0017. IGP contribution no. Xxx

## References

- Akkermans, P.M.M.G., Schwartz, G.M., 2003. The archaeology of Syria. From complex hunter-gatherers to early urban societies (ca. 16,000-300 BC). Cambridge World Archaeology, Cambridge University Press, New York, 467 pp.
- Bader, N., 1989. Earliest Cultivators in Northern Mesopotamia. The Investigations of Soviet Archaeological Expedition in Iraq at Settlements Tell Magzaliya, Tell Sotto, Kül Tepe. Moscow, Nauka.
- Bader, N., Le Mièrè, M., 2013. From pre-Pottery Neolithic to Pottery Neolithic in the Sinjar, in Interpreting the Late Neolithic of Upper Mesopotamia. Publications on Archaeology of the Leiden Museum of Archaeology (PALMA), Brepols pub. (Turnhout, Belgium), 513-520.

- 546 Bernbeck, J., Nieuwenhuysse, O.P., 2013. Established paradigms, current disputes and  
547 emerging themes: the state of research on the Late Neolithic in Upper  
548 Mesopotamia, in *Interpreting the Late Neolithic of Upper Mesopotamia*.  
549 Publications on Archaeology of the Leiden Museum of Archaeology (PALMA),  
550 Brepols pub. (Turnhout, Belgium), 17-37.
- 551 Ben-Yosef, E., Ron, H., Tauxe, L., Agnon, A., Genevery, A., Levy, T.E., Avner, U., Najjar, M.,  
552 2008. Application of copper slag in geomagnetic archaeointensity research. *J.*  
553 *Geophys. Res.* 113, B08101. doi:10.1029/2007JB005235.
- 554 Ben-Yosef, E., Tauxe, L., Levy, T.E., Shaar, R., Ron, H., Najjar, M., 2009. Geomagnetic  
555 intensity spike recorded in high resolution slag deposit in southern Jordan. *Earth*  
556 *Planet. Sci. Lett.* 287, 529-539.
- 557 Berger, J.-F., Guilaine, J., 2009. The 8200 calBP abrupt environmental change and the  
558 Neolithic transition: A Mediterranean perspective. *Quaternary Int.* 200, 31-49.
- 559 Burakov, K.S., Galyagin, D.K., Nachasova, I.E., Reshetnyak, M. Yu., Sokolov, D.D., Frick,  
560 P.G., 1998. Wavelet analysis of geomagnetic field intensity for the past 4000 years.  
561 *Izvestiya Phys. of Solid Earth* 34 (9), 773-778.
- 562 Campbell, S., 2007. Rethinking Halaf chronology. *Paléorient* 33, 103-136.
- 563 Campbell, S., Fletcher, A., 2010. Questioning the Halaf-Ubaid Transition. In: *Beyond the*  
564 *Ubaid: Transformation and integration in the late prehistoric societies of the*  
565 *Middle East*, R.A. Carter and G. Philip eds., SAOC: Studies in Ancient Oriental  
566 *Civilization* 63, The Oriental Institute of the University of Chicago, 69-83.
- 567 Coe, R. S., 1967. Paleo-Intensities of the Earth's magnetic field determined from Tertiary  
568 and Quaternary Rocks. *J. Geophys. Res.* 72, 3247-3262.
- 569 Cruells, W., Nieuwenhuysse, O., 2004. The proto-Halaf period in Syria. New sites, new  
570 data. *Paléorient* 30, 47-68.
- 571 Day, R., Fuller, M., Schmidt, V., 1977. Hysteresis properties of titanomagnetites: grain  
572 size and composition dependence. *Phys. Earth Planet. Inter.* 13, 260-267.
- 573 De Marco, E., Spatharas, V., Gomez-Paccard, M., Chauvin, A., Kondopoulou, D., 2008. New  
574 archeointensity results from archeological sites and variations of the geomagnetic  
575 field intensity for the last 7 millennia in Greece. *Phys. Chem. Earth* 33, 578-595.

- 576 Dunlop, D.J., 2002a. Theory and application of the Day plot (Mrs/Ms versus Hcr/Hc) 1.  
577       Theoretical curves and tests using titanomagnetite data. *J. Geophys. Res.* 107, 2056,  
578       10.1029/2001JB000486.
- 579 Dunlop, D.J., 2002b. Theory and application of the Day plot (Mrs/Ms versus Hcr/Hc) 2.  
580       Application to data for rocks, sediments, and soils. *J. Geophys. Res.* 107, 2057,  
581       10.1029/2001JB000487.
- 582 Ertepinar, P., Langereis, C.G., Biggin, A.J., Frangipane, M., Matney, T., Ökse, T., Engin, A.,  
583       2012. Archaeomagnetic study of five mounds from Upper Mesopotamia between  
584       2500 and 700 BC: further evidence for an extremely strong geomagnetic field ca.  
585       3000 years ago. *Earth Planet. Sci. Lett.* 357-358, 84-98.
- 586 Gallet, Y., Le Goff, M., 2006. High-temperature archeointensity measurements from  
587       Mesopotamia. *Earth Planet. Sci. Lett.* 241, 159-173.
- 588 Gallet, Y., Genevey, A., Le Goff, M., Fluteau, F., Eshraghi, S.A., 2006. Possible impact of the  
589       Earth's magnetic field on the history of ancient civilizations. *Earth Planet. Sci. Lett.*  
590       246, 17-26.
- 591 Gallet, Y., Le Goff, M., Genevey, A., Margueron, J., Matthiae, P., 2008. Geomagnetic field  
592       intensity behavior in the Middle East between 3000 BC and 1500 BC. *Geophys. Res.*  
593       Lett. 35, L02307. doi: 10.1029/2007GL031991.
- 594 Gallet, Y., Genevey, A., Le Goff, M., Warmé, N., Gran-Aymerich, J., Lefèvre A., 2009a. On the  
595       use of archeology in geomagnetism, and vice-versa: Recent developments in  
596       archeomagnetism. *C. R. Physique* 10, 630-648.
- 597 Gallet, Y., Hulot, G., Chulliat, A., Genevey, A., 2009b. Geomagnetic field hemispheric  
598       asymmetry and archeomagnetic jerks. *Earth Planet. Sci. Lett.* 284, 179-186.
- 599 Gallet, Y., D'Andrea, M., Genevey, A., Pinnock, F., Le Goff, M., Matthiae, P., 2014.  
600       Archaeomagnetism at Ebla (Tell Mardikh, Syria). New data on geomagnetic field  
601       intensity variations in the Near East during the Bronze Age. *J. Archaeol. Sci.* 42,  
602       295-304.
- 603 Gallet, Y., Butterlin, P., 2014. Archaeological and geomagnetic implications of new  
604       archaeomagnetic intensity data from the Early Bronze high terrace "Massif Rouge"



- 605 at Mari (Tell Hariri, Syria). Archaeometry online 5 June 2014, doi:  
606 10.1111/arcm.12112.
- 607 Gallet, Y., Al Maqdissi, M., 2010. Archéomagnétisme à Mishirfeh-Qatna: Nouvelles  
608 données sur l'évolution de l'intensité du champ magnétique terrestre au Moyen-  
609 Orient durant les derniers millénaires. *Akkadica* 131, 29-46.
- 610 Genevey, A., Gallet, Y., 2002. Intensity of the geomagnetic field in Western Europe over  
611 the past 2000 years: New data from ancient French pottery. *J. Geophys. Res.* 107,  
612 B11.
- 613 Genevey, A., Gallet, Y., Margueron, J., 2003. Eight thousand years of geomagnetic field  
614 intensity variations in the eastern Mediterranean. *J. Geophys. Res.* 108, 2228.  
615 doi:10.1029/2001JB001612.
- 616 Genevey, A., Gallet, Y., Constable, C., Korte, M., Hulot, G., 2008. ArcheoInt: An upgraded  
617 compilation of geomagnetic field intensity data for the past ten millennia and its  
618 application to the recovery of the past dipole moment. *Geochem. Geophys. Geosyst.*  
619 9(4), Q04038. doi: 10.1029/2007GC001881.
- 620 Genevey, A., Gallet, Y., Rosen, J., Le Goff, M., 2009. Evidence for rapid geomagnetic field  
621 intensity variations in Western Europe over the past 800 years from new  
622 archeointensity French data. *Earth Planet. Sci. Lett.* 284, 132-143.  
623 doi:10.1016/j.epsl.2009.04.024.
- 624 Genevey, A., Gallet, Y., Thébault, E., Jesset, S., Le Goff, M., 2013. Geomagnetic field  
625 intensity variations in Western Europe over the past 1100 years. *Geochem.*  
626 *Geophys. Geosyst.* 14/8, 2858-2872
- 627 Gómez, A., 2011. Caracterización del producto cerámico en las comunidades neolíticas  
628 de mediados del VI milenio cal BC: el valle del Éufrates y el valle del Khabur en el  
629 Halaf Final. PhD Thesis, Universitat Autònoma de Barcelona, Spain.
- 630 Hartmann, G., Genevey, A., Gallet, Y., Trindade, R., Etchevarne, C., Le Goff, M., Afonso, M.,  
631 2010. Archeointensity in Northeast Brazil over the past five centuries. *Earth*  
632 *Planet. Sci. Lett.* 296, 340-352.
- 633 Hartmann, G., Genevey, A., Gallet, Y., Trindade, R., Le Goff, M., Najjar, R., Etchevarne, C.,  
634 Afonso, M., 2011. New historical archeointensity data from Brazil : Evidence for a

- 635 large regional non-dipole field contribution over the past few centuries. Earth  
636 Planet. Sci. Lett. 306, 66-76.
- 637 Hong, H., Yu, Y., Lee, C.H., Kim, R.H., Park, J., Doh, S.-J., Kim, W., Sung, H., 2013. Globally  
638 strong geomagnetic field intensity circa 3000 years ago. Earth Planet. Sci. Lett. 383,  
639 142-152.
- 640 Hours, F., Aurenche, O, Cauvin, J., Cauvin, M.C., Copeland, L., Sanlaville, P., 1994. Atlas des  
641 sites du Proche-Orient (14000-5700 BP). Travaux de la Maison de l'Orient  
642 Méditerranéen 24, Lyon.
- 643 Hulot, G., Le Mouél, J.-L., 1994. A statistical approach to the Earth' s main magnetic field.  
644 Phys. Earth Planet. Inter. 82, 167-183.
- 645 Knudsen, M. Riisager, P., Donadini, F., Snowball, I., Muscheler, R., Korhonen, K., Pesonen,  
646 L., 2008. Variations in geomagnetic dipole moment during the Holocene and the  
647 past 50 kyr. Earth Planet. Sci. Lett. 272, 319-329.
- 648 Korhonen, K., Donadini, F., Riisager, P., Pesonen, L.J., 2008. GEOMAGIA50: An  
649 archeointensity database with PHP and MySQL. Geochem. Geophys. Geosyst. 9,  
650 Q04029.
- 651 Korte, M., Donadini, F., Constable, C., 2009. Geomagnetic field for 0-3 ka: 2. A new series  
652 of time-varying global models. Geochem. Geophys. Geosyst. 10, Q06008.
- 653 Korte, M., Constable, C., Donadini, F., Holme, R., 2011. Reconstructing the Holocene  
654 geomagnetic field. Earth Planet. Sci. Lett. 312, 497-505.
- 655 Kostadinova-Avramova, M., Kovacheva, M., Boyadzhiev, Y., 2014. Contribution of  
656 stratigraphic constraints of Bulgarian prehistoric multilevel tells and a comparison  
657 with archaeomagnetic observations. J. Archaeol. Sci. 43, 227-238.
- 658 Kovacheva, M., Kostadinova-Avramova, M., Jordanova, N., Lanos, P., Boyadziev, Y., 2014.  
659 Extended and revised archaeomagnetic database and secular variation curves from  
660 Bulgaria for the last eight millennia. Phys. Earth Planet. Inter. In press, doi:  
661 10.1016/j.pepi.2014.07.002.
- 662 Le Goff, M., Gallet, Y., 2004. A new three-axis vibrating sample magnetometer for  
663 continuous high-temperature magnetization measurements: applications to paleo-  
664 and archeo-intensity determinations. Earth Planet. Sci. Lett. 229, 31-43.

- 665 Le Mière, M., Picon, M., 1998. Les débuts de la céramique du Proche-Orient. *Paléorient*  
666 24/2, 27-48.
- 667 Licht, A., Hulot, G., Gallet, Y., Thébault, E., 2013. Ensembles of low degree archeomagnetic  
668 field models for the past three millennia. *Phys. Earth Planet. Inter.* 224, 38-67.
- 669 Livermore, P.W., Fournier, A., Gallet, Y., 2014. Core-flow constraints on extreme  
670 archeomagnetic intensity changes, *Earth Planet. Sci. Lett.* 387, 145-156
- 671 Masetti-Rouault, M.-G., 2005. Mission archéologique française à Tell Masaikh, projet  
672 Terqa et sa région. Rapport préliminaire de la mission 2005 à Tell Masaikh", p. 1-  
673 12.
- 674 Masetti-Rouault, M.-G., 2006. Rapporto preliminare sui lavori della missione nel sito di  
675 Tell Masaikh nel 2005 (MK10). In : Rouault O. et Mora C., Progetto Terqa e la sua  
676 regione (Siria). Rapporto preliminare 2005, *Athenaeum* fasc. 2, p. 749-756.
- 677 Masetti-Rouault, M.-G., . Rural Economy and Steppe Management in an Assyrian Colony  
678 in the West. A view from Tell Masaikh Lower Middle Euphrates, Syria. In: H. Kühne  
679 ed. *Dur-Katlimmu 2008 and Beyond*, *Studia Chaburensia*, vol. 1, Harrassowitz  
680 Verlag, 130-149.
- 681 McIntosh, G., Kovacheva, M., Catanzariti, G., Osete, M.L., Casas, L., 2007. Widespread  
682 occurrence of a novel high coercivity, thermally stable, low unblocking  
683 temperature magnetic phase in heated archeological material. *Geophys. Res. Lett.*  
684 34, L21302.
- 685 McIntosh, G., Kovacheva, M., Catanzariti, G., Donadini, F., Lopez, M.L.O., 2011. High  
686 coercivity remanence in baked clay materials used in archeomagnetism. *Geochem.*  
687 *Geophys. Geosyst.* 12, Q02003, doi:10.1029/2010GC003310.
- 688 Molist, M., 1996 (ed.). Tell Halula (Siria). Un yacimiento neolítico del valle medio del  
689 Éufrates. Campañas de 1991 y 1992. Ediciones del Ministerio de Educación y  
690 Ciencia, Madrid Spain, 223 p.
- 691 Molist, M., 1998. Espace collectif et domestique dans le néolithique des IXème et VIIIème  
692 millénaires B.P. au nord de la Syrie: apports du site de Tell Halula (Vallée de  
693 l'Euphrate), in *Espace Naturel, Espace Habité en Syrie du Nord*. (10e-2e millénaires  
694 av. J. C.). M. Fortin and O. Aurenche eds., 115-130, Québec-Lyon, BCSMS-TMO.

- 695 Molist, M., Faura, J.M., 1999. Tell Halula: Un village des premiers agriculteurs-éleveurs  
696 dans la Vallée de l'Euphrate, in *Archaeology of the Upper Syrian Euphrates. The*  
697 *Tishrin Dam Area*, Del Olmo, G. and Montero J. L. (eds.), *Proceedings of the*  
698 *International Symposium held at Barcelona, January 28-30 1998*, Ed. AUSA,  
699 Sabadell: 27-40.
- 700 Molist, M., 2001. Halula, village néolithique en Syrie du Nord, in *Communautés*  
701 *villageoises du Proche-Orient à l'Atlantique (8000-2000 av. J.-C.)*, Guilaine J. (ed),  
702 115-130, Paris, Editions Errance.
- 703 Molist, M., Anfruns, J., Borrell, F., Clop, X., Cruells, W., Gómez, A., Guerrero, E., Tornero, C.,  
704 Sana, M., 2007. Tell Halula (vallée de l'Euphrate, Syrie): nouvelles données sur les  
705 occupations Néolithiques. *Notices préliminaires sur les travaux 2002-2004*. In *Les*  
706 *résultats du programme de formation à la sauvegarde du patrimoine culturel de*  
707 *Syrie*, Abdul Massih J. (ed.), 21-52, Damas: Ministère de la culture, Direction  
708 générale des antiquités et des musées (Documents d'archéologie syrienne 11).
- 709 Molist, M., Anfruns, J., Bofill, M., Borrell, F., Buxó, R., Clop, X., Cruells, W., Faura, J.M.,  
710 Ferrer, A., Gómez, A., Guerrero, E., Saña, M., Tornero, C. & Vicente, O., 2013. Tell  
711 Halula (Euphrates Valley, Syria): New approach to VII and VI millennia cal. B.C. in  
712 Northern Levant framework, in *Interpreting the Late Neolithic of Upper*  
713 *Mesopotamia. Publications on Archaeology of the Leiden Museum of Archaeology*  
714 (PALMA), Brepols pub. (Turnhout, Belgium), 443-455.
- 715 Nachasova, I., Burakov, K., 1995. Archaeointensity of the geomagnetic field in the fifth  
716 millennium B.C. in northern Mesopotamia. *Geomagn. Aeron.* 35, 398-402.
- 717 Nachasova, I., Burakov, K., 1998. Geomagnetic variations in the VI-V millennia B.C.  
718 *Geomagn. Aeron.* 38, 502-505.
- 719 Nieuwenhuyse, O., Akkermans, P., van der Plicht, J., 2010. Not so coarse, nor always plain  
720 -the earliest pottery of Syria. *Antiquity* 84, 71-85.
- 721 Nieuwenhuyse, O.P., Bernbeck, R., Akkermans, P.M.M.G., Rogasch, J., 2013. Interpreting  
722 the Late Neolithic of Upper Mesopotamia, *Publications on Archaeology of the*  
723 *Leiden Museum of Archaeology (PALMA)*, Brepols pub. (Turnhout, Belgium), 520  
724 pp.

- 725 Nilsson, A., Snowball, I., Muscheler, R., Uvo, C.B., 2010. Holocene geocentric dipole tilt  
726 model constrained by sedimentary paleomagnetic data. *Geochem. Geophys.*  
727 *Geosyst.* 11, Q08018.
- 728 Nilsson, A., Holme, R., Korte, M., Suttie, N., Hill, M., 2014. Reconstructing Holocene  
729 geomagnetic field variation: New methods, models and implications, *Geophys. J.*  
730 *Int.* in press.
- 731 Nishiaki, Y., Le Mièrè, M., 2005. The oldest pottery Neolithic of Upper Mesopotamia: New  
732 evidence from Tell Seker al-Aheimar, the Khabur, northeast Syria. *Paléorient* 31,  
733 55-68.
- 734 Pavón-Carrasco, F.J., Osete, M.L., Torta, J.M., De Santis, A., 2014. A geomagnetic field  
735 model for the Holocene based on archaeomagnetic and lava flow data. *Earth*  
736 *Planet. Sci. Lett.* 388, 98-109.
- 737 Robert, B., Blanc, C., Chapoulie, R., Masetti-Rouault, M.-G., 2008. Characterizing the Halaf-  
738 Ubaid Transitional Period by Studying Ceramic from Tell Masatkh, Syria.  
739 Archaeological Data and Archaeometry Investigations. In : H. Kühne, R.M. Czichon,  
740 F.J. Kreppner (eds.), *Social and Cultural Transformation : The Archaeology of the*  
741 *Transitional Periods and Dark Ages Excavation Reports (Vol. 2)*, Proceedings of the  
742 4th International Congress of Archaeology of the Near East, 29 March - 3 April  
743 April 2004, Freie Universität Berlin, Harrassowitz Verlag, Wiesbaden, 225-234.
- 744 Robert, B., 2009. Production céramique et représentations animales à l'époque de Halaf.  
745 *Res Antiquae* 6, 271-292.
- 746 Robert, B., 2010. Développement et disparition de la production céramique halafienne:  
747 implications techniques et sociales à partir d'études de cas. PhD thesis Université  
748 Lumière Lyon 2, pp. 899.
- 749 Shaar, R., Ben-Yosef, E., Ron, H., Tauxe, L., Agnon, A., Kessel, R., 2011. Geomagnetic field  
750 intensity: How high can it get? How fast can it change? Constraints from Iron-Age  
751 copper-slag. *Earth Planet. Sci. Lett.* 301, 297-306.
- 752 Shaar, R., Tauxe, L., Ben-Yosef, E., Kassianidou, V., Lorentzen, B., Feinberg, J.M., Levy, T.E.,  
753 2014. Decadal-scale variations in geomagnetic field intensity from ancient Cypriot  
754 slag mounds. *Geochem. Geophys. Geosyst.* In press.

- 755 Tema, E., Kondopoulou, D., 2011. Secular variation of the Earth's magnetic field in the  
756 Balkan region during the last eight millennia based on archaeomagnetic data.  
757 *Geophys. J. Int.* 186(2), 603-614.
- 758 Thébault, E., Gallet, Y., 2010. A bootstrap algorithm for deriving the archeomagnetic field  
759 intensity variation curve in the Middle East over the past 4 millennia BC. *Geophys.*  
760 *Res. Lett.* 37, L22303. Doi:10.1029/2010GL044788.
- 761 Thellier, E., Thellier, O., 1959. Sur l'intensité du champ magnétique terrestre dans le  
762 passé historique et géologique. *Ann. Géophys.* 15, 285-376
- 763 Tsuneki, A., Miyake, Y., 1996. The earliest pottery sequence of the Levant: New data from  
764 Tell el-Kerkh 2, Northern Syria. *Paléorient* 22, 109-123.
- 765 Usoskin, I.G., Hulot, G., Gallet, Y., Roth, R., Licht, A., Joos, F., Kovaltsov, G.A., Thébault, E.,  
766 Khokhlov, A., 2014. Evidence for distinct modes of solar activity. *Astronomy &*  
767 *Astrophysics* 562, L10.
- 768 Valet J.-P., Herrero-Bervera, E. Le Mouél, J.-L., Plénier, G., 2008. Secular variation of the  
769 geomagnetic dipole during the past 2000 years. *Geochem. Geophys. Geosyst.* 9,  
770 Q01008.
- 771 Van der Plicht, J., Akkermans, P.M., Nieuwenhuyse, O.P., Kaneda, A., Russell, A.L., 2011.  
772 Tell Sabi Abyad, Syria: radiocarbon chronology, cultural change, and the 8.2 ka  
773 event. *Radiocarbon* 53(2), 229-243.
- 774 Yu, Y., Tauxe, L., Genevey, A., 2004. Toward an optimal geomagnetic field intensity  
775 determination technique. *Geochem. Geophys. Geosyst.* 5(2), Q02H07.
- 776

## Table caption

**Table 1.** Pottery group-mean intensity values obtained at Tell Halula ( $\lambda=36^{\circ}25'N$ ,  $\phi=38^{\circ}10'E$ ; pottery groups SY127 to SY132) and Tell Masaikh ( $\lambda=34^{\circ}25'N$ ,  $\phi=40^{\circ}01'E$ ; pottery groups SY37 and SY38). Information on the different archeological dating, relative chronology and references are provided in the second, third and fourth columns. See text for references on absolute dating (fifth column). \* indicates that an approximation was made on the dating (see text). The mean intensity values and their standard deviations are provided in column 6. Column 7 shows the number Nb of fragments (/n specimens) retained for computing the pottery group-mean intensity values.

## Figure captions

**Fig. 1.** (a) Location of the two Syrian archeological sites studied herein (Tell Halula and Tell Masaikh) and of three other sites discussed in the text (Tell Halaf, Yarim Tepe II and Tell Sotto). ©Google Earth. (b) General view of the Tell Halula archeological site. © Universitat Autònoma de Barcelona (UAB)/SAPPO.

**Fig. 2.** Examples of pottery sherds discovered at Tell Halula. These fragments are dated to phases I, II and III of the pre-Halaf (photos 1-2, 3-4 and 5-6, respectively), to the proto-Halaf (photos 7-8), and to the Early, Middle and Late Halaf (photos 9, 10-11 and 12-13, respectively). © Universitat Autònoma de Barcelona (UAB)/SAPPO.

**Fig. 3.** Triaxe intensity data obtained for two specimens from Tell Halula (SY89-08, SY140-06). (a,c) Thermal demagnetization data; (b,d) Triaxe measurement series; (e) Archeointensity results at the specimen level. See text and further explanations in Le Goff and Gallet (2004).

**Fig. 4.** (a) Normalized IRM acquisition curves obtained for one fragment from each time level. (b-c) Two examples of hysteresis loop. (d-g) Four examples of normalized thermomagnetic low-field susceptibility (heating and cooling) curves obtained from fragments collected at Tell Halula. These fragments are dated to the pre-Halaf (d,e), Middle Halaf (f) and to the Late Halaf (g). (h) Hysteresis ratios ( $M_{RS}/M_S$  vs.  $H_{CR}/H_C$ ) obtained at Tell Mardikh/Ebla (grey color, Gallet et al., 2014), Tell Masaikh (blue

triangles) and Tell Halula (see color code on the figure according to the archeological periods of the fragments).

**Fig. 5.** Intensity data obtained from eight different archeomagnetic pottery groups (a-e, Tell Halula; f, Tell Masaikh). Each colored curve on each of these plots shows the intensity data obtained for one specimen over the temperature range of analysis (for further explanations, see in Le Goff and Gallet, 2004). Altogether, the results from 93 specimens are hence reported in this Figure.

**Fig. 6.** Archeomagnetic field intensity variations recovered from the new data obtained at Tell Halula (blue circles) and Tell Masaikh (blue triangles). All results are converted in Virtual Axial Dipole Moments. The chronological time scale is provided in the text (see also in Table 1).

**Fig. 7.** Comparison between our new archeointensity data (in blue) and previous results obtained (a) from Yarim Tepe II and Tell Sotto (green circles and triangles, respectively), two multi-level archeological sites located in North Iraq (Nachasova and Burakov, 1995, 1998) and (b) from Bulgaria (in red; Kovacheva et al., 2014). As discussed in the text, the dating of the Yarim Tepe II and Tell Sotto data was modified from the original papers. The solid vs. open circles indicate the intensity values obtained from several vs. one specimen(s).

**Fig. 8.** Regional averaged geomagnetic field intensity variation curve in the Middle East over the past 9000 years. The data were selected inside a 1000 km-radius circle around the location  $\lambda=36^{\circ}49'N$ ,  $\varphi=40^{\circ}02'E$  (archeological site of Tell Halaf). All data were transformed into VADM. Two different approaches were successively considered to compute the curve. (a) We used sliding windows of 200 years shifted every 10 years and the bootstrap technique for taking into account the experimental and age uncertainties on the available intensity data. 1000 curves were hence computed and are shown here the mean (thick black line), the minimum and the maximum VADM values obtained for the different time windows. The Syrian data are also reported (blue dots) together with all other available archeointensity data (grey dots) satisfying minimum selection criteria (Genevey et al., 2008). (b) We used an iteratively reweighted least-squares algorithm, combined with a bootstrap, modified from that of Thébault and Gallet (2010). The



continuous black line shows the maximum of probability, and the light blue lines its 95% fluctuation envelope. The 95% confidence interval is displayed by the red lines.

**Fig. 9.** Comparison between the geomagnetic field intensity (transformed into VADM) variation curve in the Middle East, with averaging over sliding windows of 500 years (black lines; see text), and previous dipole field moment reconstructions. The comparison is made with (a) the VADM variation curve computed by Knudsen et al. (2008) using temporal and geographic averaging (in red), (b) dipole moment reconstructions derived from different time-varying global geomagnetic field modeling (blue lines, modeling proposed by Pavón-Carrasco et al., 2014; orange and green lines, the pfm9k.1b and pfm9k.1a modeling proposed by Nilsson et al., 2014).

Figure 1

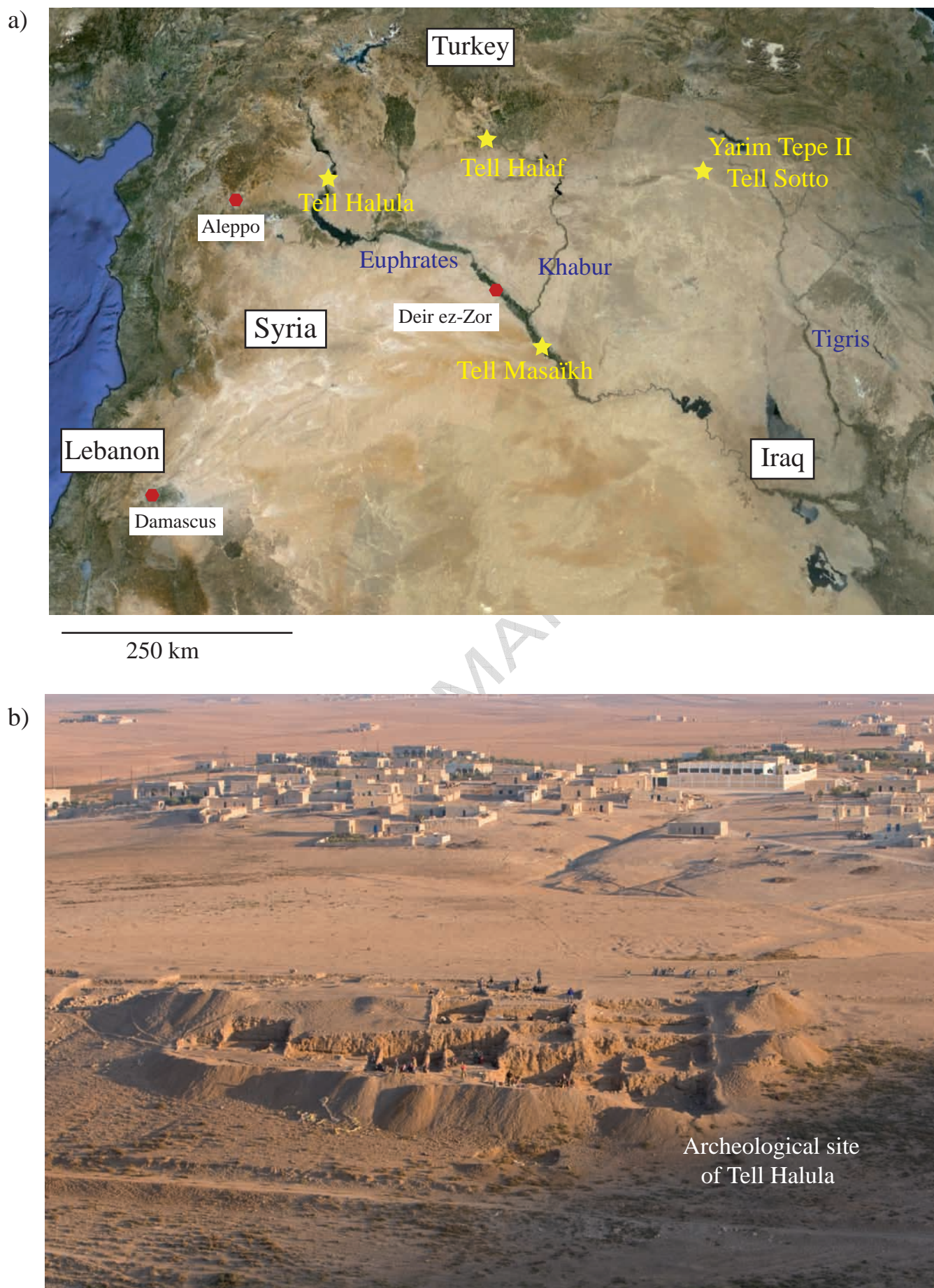


Figure 1



Figure 2

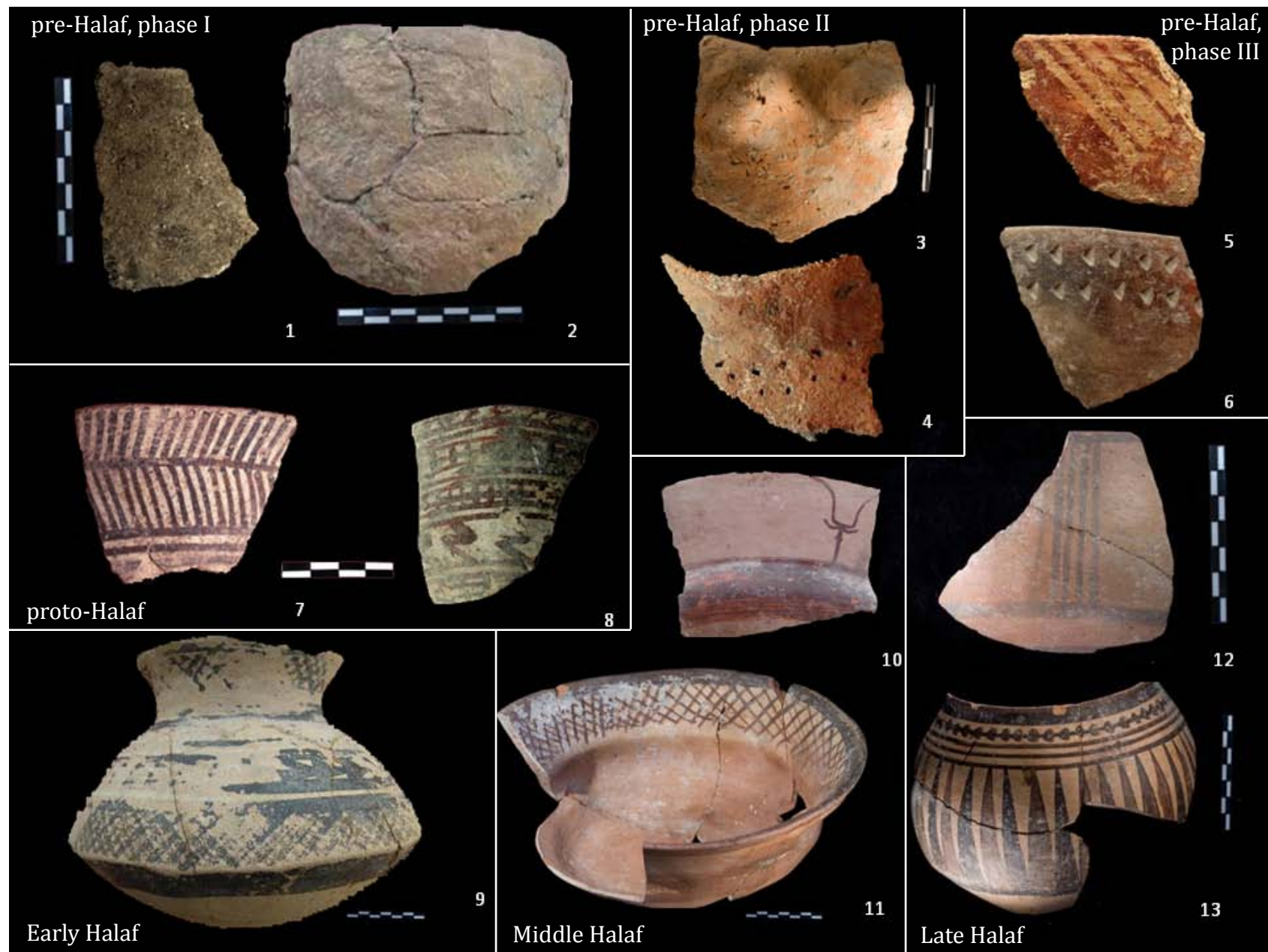


Figure 2

Figure 3

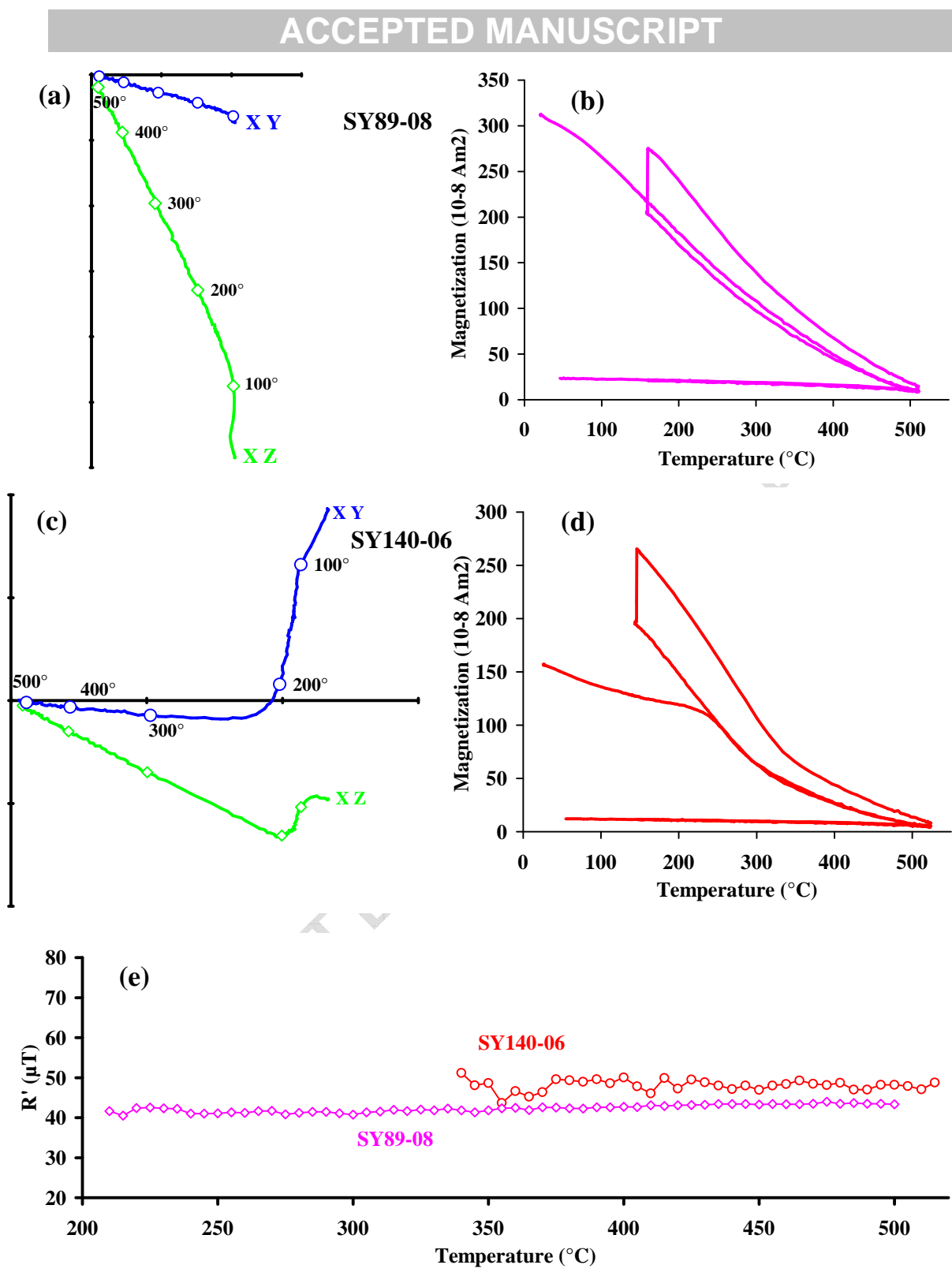
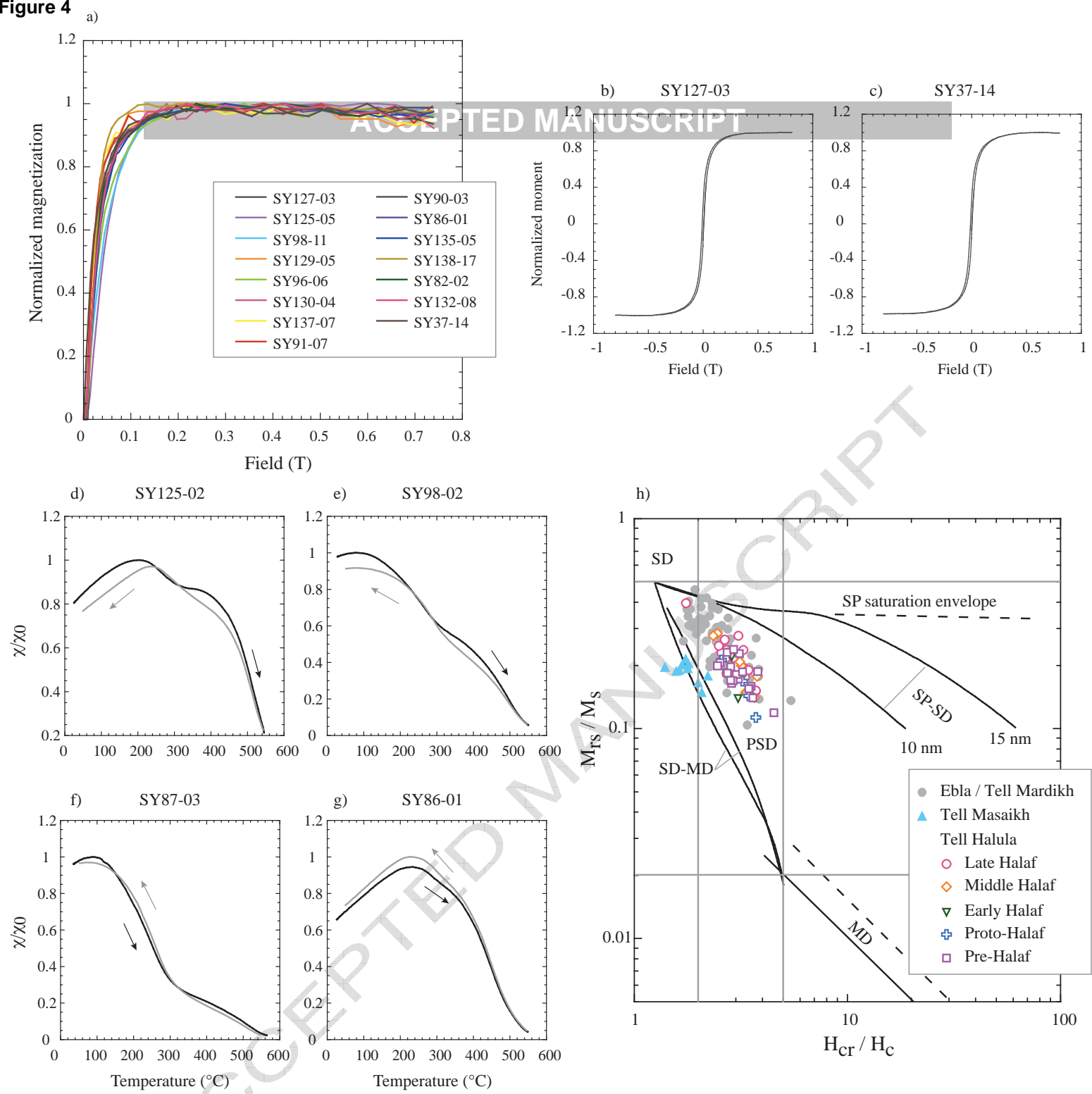
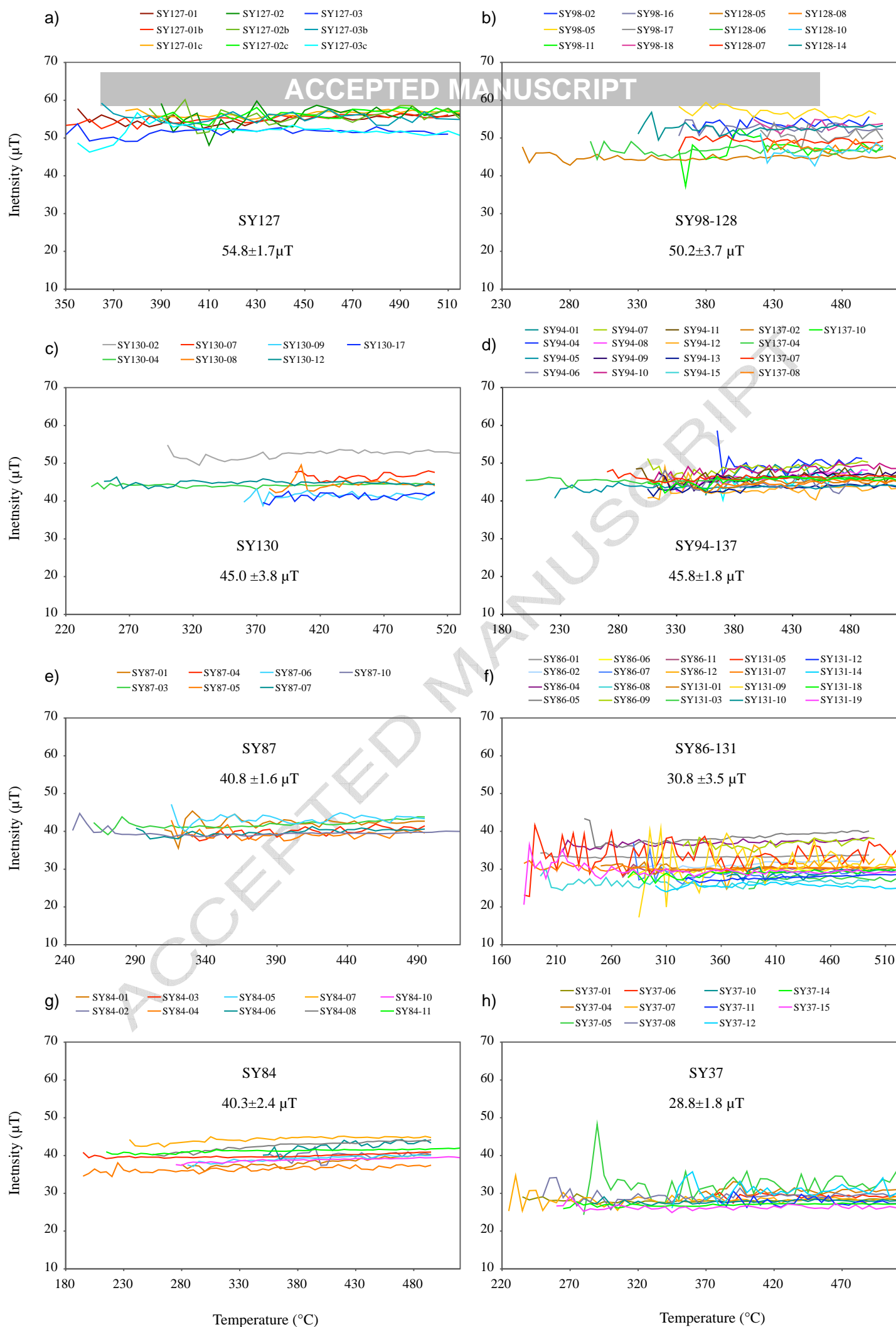


Figure 3

**Figure 4****Figure 4**

**Figure 5**



**Figure 5**

Figure 6

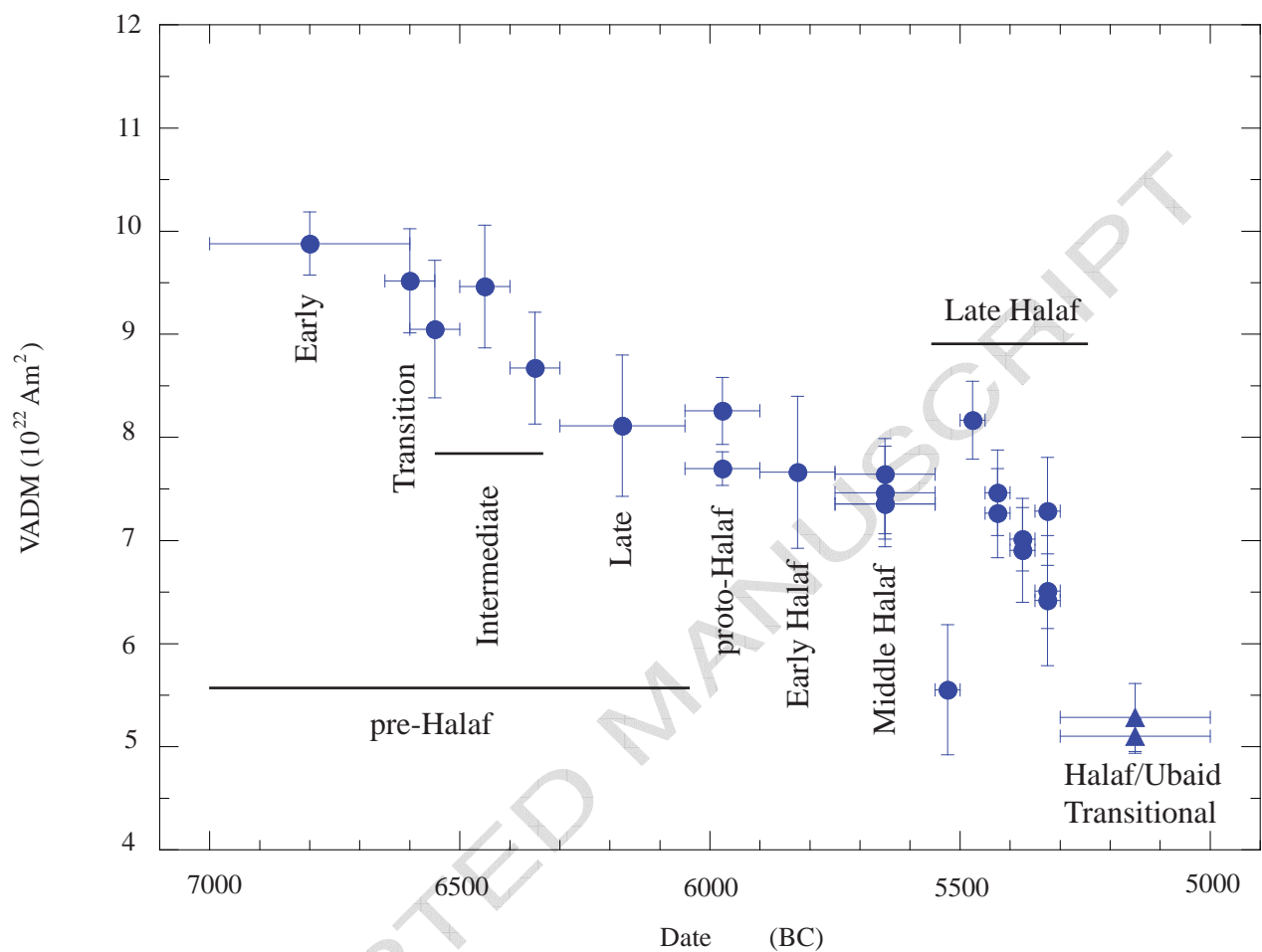


Figure 6

Figure 7

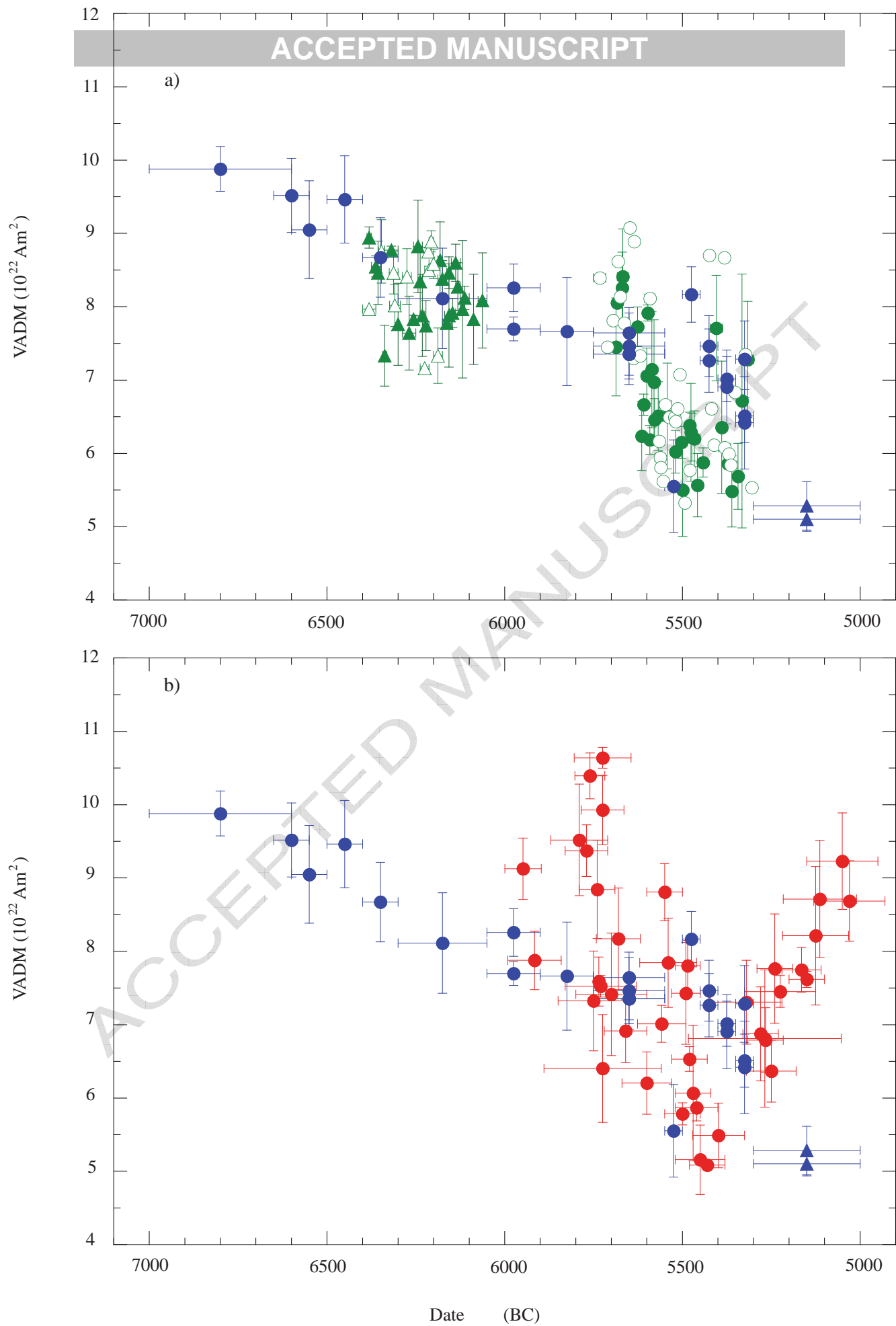


Figure 7



Figure 8

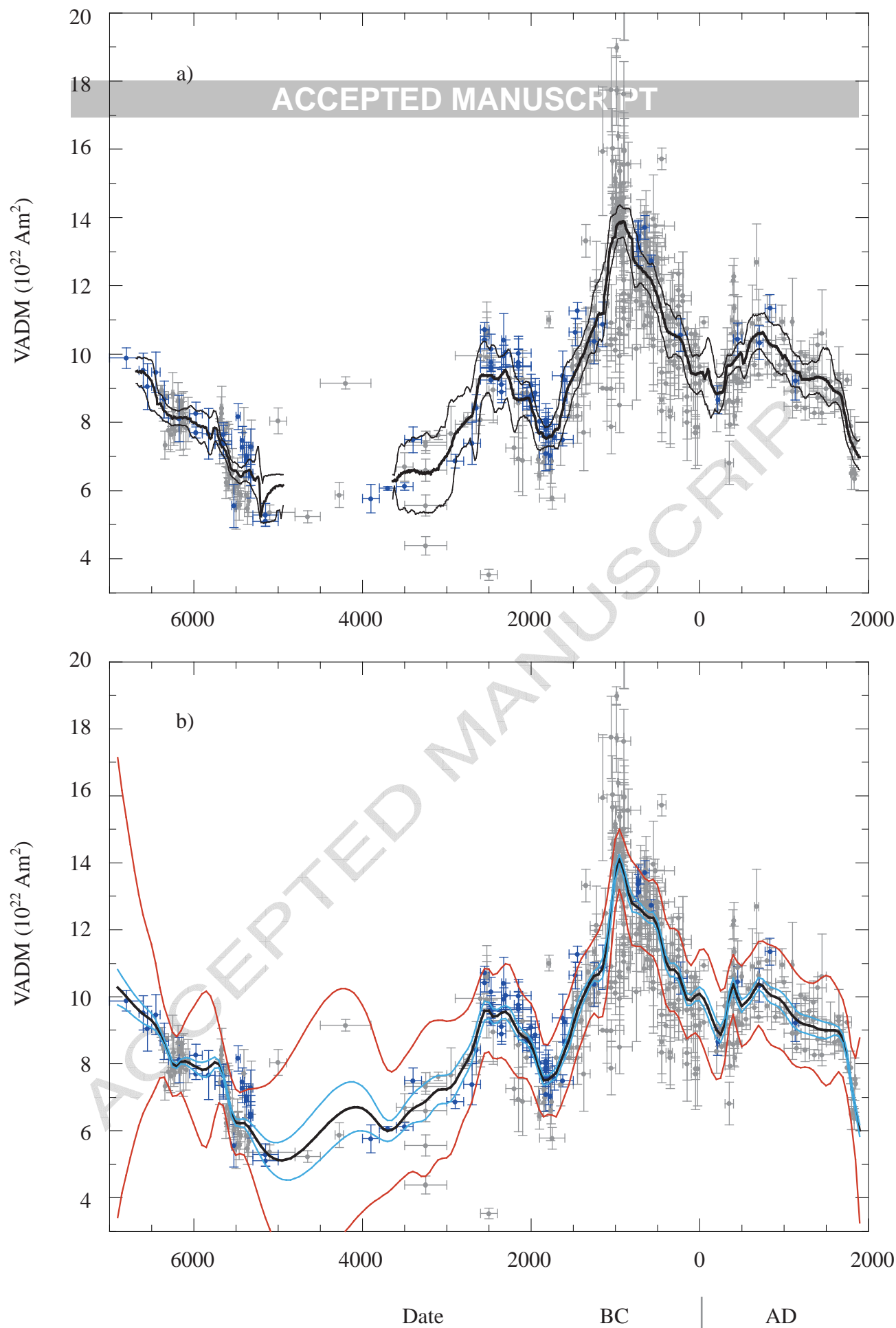


Figure 8

Figure 9

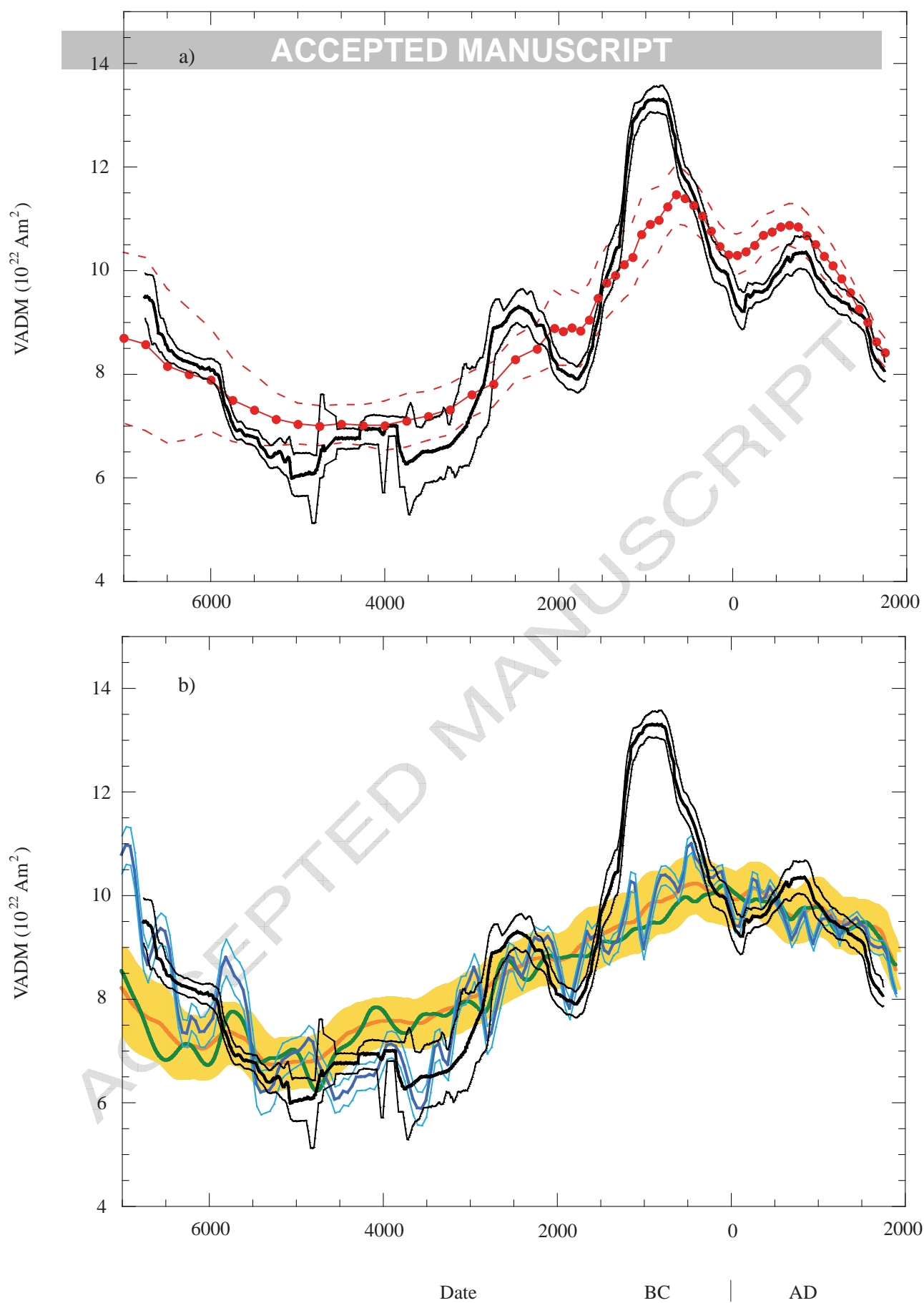


Figure 9

Pottery Group	Archeological Period	Relative chronology (Tell Halula)	Archeological reference	Age (BCE)	Intensity ( $\mu$ T)	N frag. (n spec.)
ACCEPTED MANUSCRIPT						
SY127	Early Pre-Halaf	Phase I	Sector 2, square G, peat E10	6800 $\pm$ 200	54.8 $\pm$ 1.7	3 (9)
SY125	Transition Early-Intermediate Pre-Halaf	Phase I/II	Sector 2, square I, A25	6600 $\pm$ 50	52.8 $\pm$ 2.8	2 (6)
SY98-128	Intermediate Pre-Halaf	Phase II -early phase	Sector SS14-Y, A6	6650 $\pm$ 50*	50.2 $\pm$ 3.7	12 (12)
SY97-129	Intermediate Pre-Halaf	Phase II -interm. Phase	Sector SS14-Y, A5a	6450 $\pm$ 50*	52.5 $\pm$ 3.3	17 (17)
SY96-140	Intermediate Pre-Halaf	Phase II -late phase	Sector SS14-Y, A3c	6350 $\pm$ 50*	48.1 $\pm$ 3.0	13 (13)
SY130	Late Pre-Halaf	Phase III	Sector 49, A9a, E25	6175 $\pm$ 125	45.0 $\pm$ 3.8	7 (7)
SY94-137	Proto-Halaf	Phase IV	Sector 44/3, A23, E27	5975 $\pm$ 75	45.8 $\pm$ 1.8	17 (17)
SY95	Proto-Halaf	Phase VI	Sector 40, A10	5975 $\pm$ 75	42.7 $\pm$ 0.9	5 (14)
SY91	Early Halaf	Phase V	Sector 44/4	5825 $\pm$ 75	42.5 $\pm$ 4.1	9 (9)
SY87	Middle Halaf	Phase VI	Sector 45, peat E5	5650 $\pm$ 100	40.8 $\pm$ 1.6	7 (7)
SY88	Middle Halaf	Phase VI	Sector 45, peat E9	5650 $\pm$ 100	42.4 $\pm$ 1.5	7 (7)
SY89	Middle Halaf	Phase VI	Sector 45, peat E1	5650 $\pm$ 100	40.8 $\pm$ 1.9	8 (8)
SY90	Middle Halaf	Phase VI	Sector 45, peat E3	5650 $\pm$ 100	41.4 $\pm$ 2.9	8 (8)
SY86-131	Late Halaf	Phase VII -early phase	Sector 49, A5	5525 $\pm$ 25*	30.8 $\pm$ 3.5	20 (20)
SY135	Late Halaf	Phase VII -interm./early Phase	Sector 49, A1g	5475 $\pm$ 25*	45.3 $\pm$ 2.1	11 (11)
SY84	Late Halaf	Phase VII -interm./interm. Phase	Sector 49, A1c	5425 $\pm$ 25*	40.3 $\pm$ 2.4	10 (10)
SY138	Late Halaf	Phase VII -interm./interm. Phase	Sector 49, A1c, E8	5425 $\pm$ 25*	41.4 $\pm$ 2.3	11 (11)
SY82	Late Halaf	Phase VII -interm./late Phase	Sector 49, A7	5375 $\pm$ 25*	38.3 $\pm$ 2.8	7 (7)
SY83-136	Late Halaf	Phase VII -interm./late phase	Sector 49, A1b	5375 $\pm$ 25*	38.9 $\pm$ 1.7	13 (13)
SY80	Late Halaf	Phase VII -late phase	Sector 49, A7d, peat 24	5325 $\pm$ 25*	35.6 $\pm$ 3.5	8 (8)
SY81	Late Halaf	Phase VII -late phase	Sector 49, A7c, peat 32	5325 $\pm$ 25*	36.1 $\pm$ 2.0	6 (6)
SY132	Late Halaf	Phase VII -late phase	Sector 49, A7a, E21	5325 $\pm$ 25*	40.4 $\pm$ 2.9	8 (8)
SY37	Halaf-Ubaid Transitional	-	Locus K171 I/2, layer E2	5150 $\pm$ 150	28.8 $\pm$ 1.8	11 (11)
SY38	Halaf-Ubaid Transitional	-	Locus K171 I, floor E7	5150 $\pm$ 150	27.8 $\pm$ 0.9	5 (15)

Table 1

848 New archeomagnetic intensity data from two Syrian Late Neolithic archeological sites

849

850 We recover the regional geomagnetic intensity variations between ~7000 BC and  
851 ~5000 BC

852

853 A 9000-years long archeointensity variation curve is constructed for the Middle East

854

855 We constrain the variations in the dipole field moment over most of the Holocene

856

857